Progress In Electromagnetics Research B, Vol. 26, 213–236, 2010

ARRANGING OVERHEAD POWER TRANSMISSION LINE CONDUCTORS USING SWARM INTELLIGENCE TECHNIQUE TO MINIMIZE ELECTROMAGNETIC FIELDS

M. S. H. Al Salameh and M. A. S. Hassouna

Department of Electrical Engineering
Jordan University of Science and Technology, Irbid 22110, Jordan

Abstract—Although there is no certain known mechanism of how the electromagnetic fields (EMFs) at power frequency (50/60 Hz) can affect human health, it has been epidemiologically shown that they have many hazards on human health. Also the power frequency fields may interfere with the nearby electrical and electronic equipment. In response to the precautionary principle, it might be needed in some situations to reduce the magnetic and electric fields of a high voltage line segment when it passes in close proximity to a populated area or may interfere with sensitive equipment. In other words, new arrangements of high voltage "green lines" are needed. This paper introduces a numerical solution based on Particle Swarm Optimization (PSO) technique, to reduce both magnetic and electric fields of high voltage overhead transmission line by rearranging the conductors. The horizontal, vertical, and triangular configurations of both single circuit and double circuit transmission lines were investigated. The examples presented in this paper show that the rearranged line configurations can introduce up to 81% reduction in magnetic field and up to 84% in electric field when the effects of ice and wind are considered, and up to 97% reduction in both magnetic and electric fields when these effects are neglected. A comparison is made between the cost of reducing EMFs of a line segment in a suburban area in Amman in Jordan, and the cost of not-reducing EMFs, where it is found that the cost of reducing the fields is outweighed by the "possible health costs" otherwise.

Received 21 August 2010, Accepted 13 October 2010, Scheduled 21 October 2010
Corresponding author: M. S. H. Al Salameh (salameh@just.edu.jo).

1. INTRODUCTION

With the population growth around the world, towns are expanding; many buildings become near high voltage overhead power transmission lines and many will be there very soon. This matter increases the investigations about the health effects of electromagnetic fields near the transmission lines. For example, exposure to electromagnetic fields (EMFs) at power frequency (50/60 Hz) may increase the risk of many diseases [1, 2], due to the currents induced in the human tissues, and the strength of these induced currents depends on the intensity of the outside magnetic field [3]. According to International Agency for Research on Cancer (IARC), 50 or 60 Hz magnetic fields have been classified in the list of "possibly carcinogenic" agents [4]. On the engineering side, many problems may appear in the function of electrical and electronic devices due to the interference if they are exposed to electromagnetic fields. For instance, problems could appear with medical electric equipments due to their sensitivity [5], in addition to electromagnetic interference problems caused by electric transmission and distribution lines on neighboring metallic utilities such as communication cables [6].

International Commission on Non-Ionizing Radiation Protection (ICNIRP) puts limits for electromagnetic exposure. It divides the limits into two parts: general public and occupational exposure. At 50 Hz, general public limits are 100 μT for magnetic flux density and 5 kV/m for electric field strength, whereas occupational exposure limits are 500 μT for magnetic flux density and 10 kV/m for electric field strength [7]. These limits reflect only detrimental harm as a result of short-term acute exposures which are considerably higher than 0.4 μT (4 mG); the level at which there appears to be a statistical link with a doubled risk of development of childhood leukemia, so 0.4 μT is considered as a Precautionary Principle (PP) level [4].

Many countries applied PP, and some countries like Switzerland made a bridge between the two limits by considering ICNIRP limits for dangerous health effects, and considering PP level in sensitive places such as hospitals, schools, and playgrounds [8]. Some other countries have different limits [9].

Many methods of reducing EMFs were studied in literature. For example, shielding is a common, widely used method. However, unlike RF fields which can be shielded using relatively thin conductive sheets, extremely low frequency magnetic fields are largely unaffected by the electrical conductivity of the material, unless that conductivity is high enough to produce extremely large eddy currents. Thus, shielding extremely low frequency magnetic fields can be done using

superconductors [10]. Magnetic shielding can also be done using ferromagnetic materials with high permeabilities. A shielding line may be set under the high voltage transmission line with the purpose of reducing the electric field around the houses near or beneath the transmission line. The optimum parameters of the shielding line, such as height, position, and number of lines were analyzed [25]. Accordingly, the shielding line reduces only the electric field under the line. In contrast to that, the algorithm presented in the current paper simultaneously reduces the electric and magnetic fields of the transmission line. Active shielding is another method that could be used to reduce EMFs, but its disadvantage is the need to dynamic measure of magnetic field, and dynamic adapting for the supplying current, this means additional measurement and control devices, also any error in controlling the current may form a new source of EMFs [11, 12]. Rearranging the phases is an efficient way to reduce EMFs. For example, the phases arrangement abc-cba for double circuit transmission lines is referred to as low reactance phasing (LR) and was verified to introduce up to 60% reduction in electric field over super bundles [13, 14]. Compaction can also provide reduction in EMFs. However, there are some problems, which include higher voltage gradients on conductors and insulators resulting in higher audible noise, radio interference, and increased hardware corona [15]. Rearranging the transmission line conductors to reduce only the magnetic field using PSO was verified to give good results [16].

In this paper, Particle Swarm Optimization (PSO) is used to seek the optimal transmission line conductors' arrangement which produces minimum of both magnetic and electric fields. Matlab programs were written to implement the PSO technique to minimize electromagnetic fields of different transmission line configurations. The horizontal, vertical, and triangular configurations of both single circuit and double circuit transmission lines were investigated. In these programs, PSO particles are freely moving to find any arbitrary optimal configurations in order to minimize magnetic and electric fields, and we used two models: a complex image model to calculate the magnetic field of the transmission line, and a real image model to calculate the electric field. Detailed equations and algorithm necessary to apply this method are described in this paper.

2. PARTICLE SWARM OPTIMIZATION (PSO)

Particle swarm optimization (PSO) is a stochastic, adaptive population-based nonlinear optimization algorithm that can lead to optimum solutions without knowing the gradient of the problem

beforehand. It's considered to be a number of parallel searches using a group of particles, which is suitable to solve optimization problems. It's used in our research to obtain the best configuration of the high voltage overhead transmission lines conductors which produces minimum of both magnetic and electric fields. PSO was suggested by Kennedy and Eberhart in 1995, based on the analogy of bird swarm and fish schools [17]. The main idea of PSO is summarized in finding the best result or at least acceptable one for a multidimensional optimization problem based on the movement of particles and the interactions between them by comparing the best personal solution of each particle, and the best global one using a given fitness function like bees swarm behavior in finding the most crowded position of flowers [18]. Below are definitions of PSO vocabularies and then procedures which are followed by particles to find the final results.

2.1. PSO Language

Particle: is a swarm member (a particle represents an arrangement of line conductors, and moving the particle corresponds to changing locations of conductors).

Swarm: the entire collection of particles (total group of transmission line arrangements).

Fitness function: determines optimality of a solution (equation that combines electric and magnetic field values; the lower the better).

Fitness value: a number returned from the fitness function describing how much is the goodness of the solution (minimum electric and magnetic fields).

Pbest or personal best: best solution for each particle (best conductors' locations for a particle).

Gbest or global best: best solution obtained from all the swarm by comparing all particles' pbests and selecting the one with the highest fitness function (best arrangement among all particles).

Solution space: is the range in which the particles are allowed to search, and it is determined by putting maximum and minimum locations allowed for the particles to reach (determined by minimum and maximum acceptable line heights, minimum distances between tower and conductors, and the maximum distances between conductors and tower. These values may be chosen with the help of high voltage transmission line standards, such as the IEC-71 standards).

2.2. PSO Algorithm

PSO algorithm follows the steps below:

1. Define the solution space as defined above.
2. Define fitness function (FF): In fact, we performed several trials of executing the computer programs using different expressions for FF, and we found that the following expression gave best results $\mathrm{FF} = B + 8 \times 10^{-11} E$, where B is magnetic flux density in Tesla and E is electric field in V/m. The following may shed some light on the choice of this expression. The PP (precautionary principle) limit value of B is $0.4\,\mu\mathrm{T}$, and the general public exposure limit according to ICNIRP is $5\,\mathrm{kV/m}$. If we directly add $B + E$ to obtain the FF, the PSO algorithm will be essentially based on E value only, since B value (order of micro) is much smaller than E value (order of kilo). To illustrate this, assume that after some iterations, PSO algorithm reduces E field to $4\,\mathrm{kV/m}$, and the B field to $1000\,\mu\mathrm{T}$, then direct addition of $B + E$ gives $0.001 + 4000 = 4000.001$ which is smaller than their threshold sum $0.4 \times 10^{-6} + 5000$, and consequently the program will stop with this unwanted large value of B! To overcome this, we thought to reduce the weight of E by multiplication by a small number which would equalize the values of B and weighted E in the fitness function (FF) when the corresponding threshold values of the B and E fields are substituted. Accordingly, we want (weight)(E threshold) = (B threshold), i.e., (weight)(5000) = (0.4×10^{-6}), this gives weight = 8×10^{-11}. In view of that, the threshold value of FF is 0.8×10^{-6}. In case the threshold value is not reached, the algorithm will stop at the maximum number of iterations (chosen to be 1000 iterations, based on trials for many configurations of transmission lines).
3. Initialize position and velocity for each particle in the swarm. In double circuit transmission line with 6 conductors, the position of particle (conductors' arrangement) i is represented by the positions of its 6 conductors: $X_i = [x_{i1}, x_{i2}, x_{i3}, x_{i4}, x_{i5}, x_{i6}]$, $Y_i = [y_{i1}, y_{i2}, y_{i3}, y_{i4}, y_{i5}, y_{i6}]$, where x is x-coordinate and y is y-coordinate of each conductor. Similarly, the velocity of particle i is represented by: $V_{xi} = [v_{xi1}, v_{xi2}, v_{xi3}, v_{xi4}, v_{xi5}, v_{xi6}]$ and $V_{yi} = [v_{yi1}, v_{yi2}, v_{yi3}, v_{yi4}, v_{yi5}, v_{yi6}]$, where x, y indicate the x- and y-components of the velocity of each conductor in particle i. We used a swarm of 49 particles; using 7 variations in the x-direction by 7 variations in y-direction of the conductors' positions. Lower number of particles, such as 36, yielded optimized solutions as well. However, we have chosen a higher number of 49 since the execution time of the programs is a fraction of a second.
4. Move particles throughout the solution space using the following equations for updating the position and velocity of each conductor

d in each particle i. The following equations are based on equations given by [19, 20]. For double circuit line, d is assumed $1, 2, \ldots, 6$, whereas d has the values 1, 2, 3 for single circuit line.

$$x_{id}^{t} = x_{id}^{t-1} + v_{x,\,id}^{t}\,\Delta t \tag{1}$$

$$y_{id}^{t} = y_{id}^{t-1} + v_{y,\,id}^{t}\,\Delta t \tag{2}$$

$$\begin{aligned} v_{x,\,id}^{t} = {} & K\left[v_{x,\,id}^{t-1} + c_{11} r_{x1}^{t}\left(x_{Pbest,id}^{t} - x_{id}^{t-1}\right)\right. \\ & \left. + c_{21} r_{x2}^{t}\left(x_{Gbest,d}^{t} - x_{id}^{t-1}\right)\right] \end{aligned} \tag{3}$$

$$\begin{aligned} v_{y,id}^{t} = {} & K\left[v_{y,id}^{t-1} + c_{11} r_{y1}^{t}\left(y_{Pbest,id}^{t} - y_{id}^{t-1}\right)\right. \\ & \left. + c_{21} r_{y2}^{t}\left(y_{Gbest,d}^{t} - y_{id}^{t-1}\right)\right] \end{aligned} \tag{4}$$

where $K = 0.729$, $c_{11} = c_{21} = 2.05$, and the superscripts t, $t-1$ refer to the current and previous values, respectively. The subscripts i, d refer to particle (conductors' arrangement) number and conductor number, respectively. The subscripts *Pbest, Gbest* indicate personal best and global best, respectively. Thus, v_{id}^{t} is the current velocity of dth conductor in particle i. r_{x1}^{t}, r_{x2}^{t}, r_{y1}^{t}, r_{y2}^{t}: random uniformly distributed numbers in the range $[0, 1]$, used to maintain diversity of the population. It is worth mentioning that r_{x1}^{t}, r_{x2}^{t},r_{y1}^{t}, r_{y2}^{t} were simply implemented by the built-in random number generator (rand) in the Matlab. Each time rand is activated it will give randomly a different number between $(0, 1)$. For the constant c_{11} and c_{21}, if low values are chosen, the particles will roam far from the target region before being tugged back, and if high values are chosen, the particles will move abruptly toward or past the target region. By trial and error, the best choice is to consider $c_{11} = c_{21} = 2.05$ which approximately equals the value given in the literature [28]. The constriction factor K which improves PSO's ability to control velocities is given as: $K = 2/\left|2 - c - \sqrt{c^2 - 4c}\right|$, where $c = c_{11} + c_{21} = 2.05 + 2.05 = 4.1$, resulting in $K = 0.729$.

5. Evaluate the fitness function for each particle.
6. Compare the fitness function value of the current particle with pbest value. If it is smaller than pbest value, then pbest will be replaced by the position of the new solution, otherwise, current solution is discarded.
7. Compare the fitness function value of the current particle with gbest value. If it is smaller than gbest value, then gbest will be replaced by the position of the new solution, otherwise, the current solution is discarded.

8. If number of iterations reaches the maximum value (chosen to be 1000) specified in step 2, stop and output the minimized configuration.
9. If gbest value is greater than the threshold value (chosen to be 0.8 μT) specified in step 2, return to step 4. Otherwise, stop and output the minimized configuration.

2.3. PSO versus Genetic Algorithm

Genetic Algorithm (GA) and PSO have different principles: GA is based upon genetic encoding and natural selection, as it takes a sample of possible solutions (chromosomes) and employs mutation and crossover, whereas PSO is based upon social swarm behavior in looking for the most fertile feeding location. Each chromosome in GA is scored based on its performance; this score is usually called fitness value. Chromosomes with best scores (fitness values) are selected to be parents. Crossover is performed by causing parents to be combined together by cut and splicing to produce new chromosomes (children). These offspring chromosomes form new population, or replace some of the chromosomes in the existing population, in hope that new population will be better than previous. Mutation operation makes random but small changes to encoded solution.

In PSO, every particle remembers its own best value as well as the global best; therefore it has more effective memory capability than GA. PSO's relative robustness to control parameters and computational efficiency through manipulating of the inertial weights is more than what happens in GA by crossover and mutation rates [26]. The algorithmic simplicity is one advantage of PSO over GA. In PSO, stagnation can be prevented using large inertial weight, which enforces particles to fly back and forth over gbest which makes it possible to find better results, while in GA if all chromosomes selected (parents) have the same code, then crossover and mutation processes will cause little or no effect, so children are nearly the same as parents, then all next generation are the same. In some cases, PSO has faster convergence rate than GA [27].

3. MAGNETIC FIELD OF OVERHEAD HIGH VOLTAGE TRANSMISSION LINE

The magnetic field around a three-phase line can be calculated by superimposing the individual contribution of the current of each phase conductor and taking into account the return currents through the earth. The magnetic field intensity at the point j is obtained by

considering the contribution of all N conductors, assuming parallel lines over a flat earth [21]. A line conductor is located at (x_i, y_i) with electric current of I_i.

$$\vec{H}_j = \sum_i^N \frac{I_i}{2\pi r_{ij}} u_{ij} + \sum_i^N \frac{-I_i}{2\pi r'_{ij}} \left(1 + \frac{1}{3}\left(\frac{2}{\gamma r'_{ij}}\right)^4\right) u'_{ij} \tag{5}$$

$$u_{ij} = \frac{y_i - y_j}{r_{ij}} u_x - \frac{x_i - x_j}{r_{ij}} u_y, \quad u'_{ij} = \frac{y_i + y_j + \frac{2}{\gamma}}{r'_{ij}} u_x - \frac{x_i - x_j}{r'_{ij}} u_y$$

$$r_{ij} = \sqrt{(x_j - x_i)^2 + (y_j - y_i)^2}, \quad r'_{ij} = \sqrt{(x_j - x_i)^2 + \left(y_j + y_i + \frac{2}{\gamma}\right)^2}$$

where $\gamma = \sqrt{j\omega\mu(\sigma + j\omega\varepsilon)}$, σ, ε, μ and ω are the conductivity, permittivity, permeability of the earth, and angular frequency, respectively. Note that r_{ij} is the distance between line conductor and field point, while r'_{ij} is the distance between the complex image of line conductor, through earth, and the field point. u_x and u_y are unit vectors along the x and y directions. The x and y directions are shown in Fig. 1. Finally, the magnetic flux density is related to magnetic field by $\vec{B} = \mu \vec{H}$. The parameter γ was introduced in Equation (5) in order to take into account the magnetically-induced earth return currents that spread out in the earth under the transmission line where the

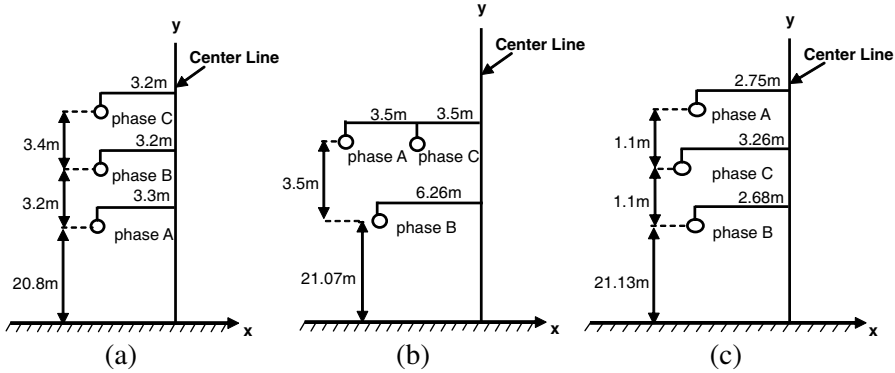

Figure 1. Conductor arrangements of 132 kV overhead vertical single circuit transmission line with 338, 312, and 310 A in phases A, B, and C respectively (Example 1). (a) Existing. (b) Optimized line with considering ice and wind effects. (c) Optimized line without considering ice and wind effects.

earth was considered as a semi-infinitely (the upper half is free space) extended non-ideal conductor.

4. ELECTRIC FIELD OF OVERHEAD HIGH VOLTAGE TRANSMISSION LINE

The electric field around a transmission line can be obtained by representing the earth effect by image charges located below the conductors at a depth equal to the conductor height, i.e., using image theory with earth considered as perfect conductor without loss of generality. Based on an equation given by [22], the electric field at a point located at (x, y) due to phase conductor A located at (x_{0A}, y_{0A}) with electric charge q_A is:

$$\vec{E}_A(x,y) = \frac{-q_A}{4\pi\varepsilon_0} \left[\frac{2(y+y_{0A})\,u_y + 2(x-x_{0A})\,u_x}{(y+y_{0A})^2+(x-x_{0A})^2} - \frac{2(y-y_{0A})\,u_y + 2(x-x_{0A})\,u_x}{(y-y_{0A})^2+(x-x_{0A})^2}\right], \quad (6)$$

where $q_A = V_{An}C_A$, $C_A = \frac{2\pi\varepsilon_0}{\ln(GMD/r_A)}$, C_A, r_A are capacitance of phase to neutral and radius of phase conductor A, ε_0 is free space permittivity, and V_{An} is the phase voltage. GMD (geometric mean distance) is the equivalent spacing between conductors; for further details about the concept of GMD, the reader is referred to [29]. Similar equations can be written for phase conductors B and C; simply by replacing the subscript A in (6) by B or C. The electric field at (x, y) due to all conductors is obtained by the superposition of the electric fields from all conductors. For single circuit transmission line: $GMD = \sqrt[3]{D_{12}D_{23}D_{13}}$ where D_{ij} is distance between phase conductors i and j. For double circuit line: $GMD = \sqrt[3]{D_{AB}D_{BC}D_{AC}}$, $D_{AB} = \sqrt[4]{D_{a1b1}D_{a1b2}D_{a2b1}D_{a2b2}}$, $D_{BC} = \sqrt[4]{D_{b1c1}D_{b1c2}D_{b2c1}D_{b2c2}}$, $D_{AC} = \sqrt[4]{D_{a1c1}D_{a1c2}D_{a2c1}D_{a2c2}}$, where one of the circuits has the three phase conductors a_1, b_1, c_1, and the other circuit has the three phase conductors a_2, b_2, c_2. Accordingly D_{aibj} is the distance between conductors a_i and b_j. Similarly, D_{bicj} is the distance between conductors b_i and c_j, and D_{aicj} is the distance between conductors a_i and c_j.

If the conductor is bundled in a single circuit transmission line, the conductor radius r_A in (6) is replaced by its equivalent geometric mean radius r_b given by $r_b = \sqrt[n]{r \times d^{(n-1)}}$ where n is the number of subconductor bundles, and d is the distance between bundles. If the conductor is bundled in a double circuit line, the conductor radius r_A in (6) is replaced by its equivalent geometric mean radius

$GMR = r_b \sqrt[3]{D_A D_B D_C}$ where D_A, D_B, D_C are distances between similar phase conductors of the two circuits. Thus, D_A is the distance between phase A conductors of the two circuits.

5. RESULTS

PSO is applied to different configurations of single circuit and double circuit lines. Each configuration has two cases of optimization, the first one is with considering the effects of ice and wind and the second one is with neglecting these effects. The magnetic and electric fields for the existing unoptimized line are compared with the optimized lines to show the reduction in both magnetic and electric fields after optimization. For all examples in this paper, the moduli of electric and magnetic fields are computed as a function of lateral (horizontal) distance (x) from the line, at $y = 1$ m height above the ground. The lateral (horizontal) distance x and vertical distance y are identified in Figs. 1, 3, 5, 7, 9, 11, and 13. The operating frequency is 50 Hz for examples 1–6, and it is 60 Hz for example 7. Before using the computer program to optimize transmission line problems, it was verified by comparison with published measured data for different configurations where excellent agreement was observed. Because the results are not the same each time we run the program, as the particles of PSO move randomly, we run the program 100 times for each transmission line problem, and we record best, average, and worst solutions. We will present here only the best solutions due to space limitations of the paper. In all the examples here, it is noted that reduction in magnetic and electric fields are larger when neglecting wind and ice effects as compared with the case of considering wind and ice effects. This may be a result of allowing shorter distances between phase conductors when neglecting wind and ice effects. The execution time of the PSO program is less than 1 second on a computer with Intel (R) Pentium (R) Dual CPU T2310@1.46 GHz, 125 GB HD, 1 GB RAM.

5.1. Example 1: Single Circuit 132 kV Vertical Line

A vertical line of 132 kV formed by three conductors arranged as shown in Fig. 1 is considered with light unbalance between phases: 338, 312, and 310 A for phases A, B, and C respectively [21]. The unoptimized (existing) and optimized lines are shown in Fig. 1. The magnetic and electric fields before and after optimization are shown in Fig. 2, where optimized lines show significant decrease in both fields as illustrated in Table 1. Note that although the existing line is vertical, the optimized lines are not vertical. Also the phase sequence is not the same for the

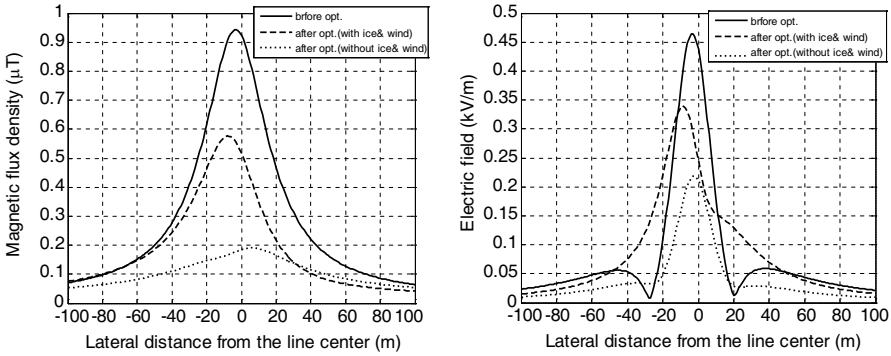

(a) Megnetic field (b) Electric field

Figure 2. Profile of magnetic and electric fields of 132 kV overhead single circuit vertical line at 1 m above the ground for the three conductor arrangments in Fig. 1 (Example 1).

three configurations in Fig. 1. This is expected because the particles in the PSO swarm move freely within the solution space. So, it is not only the distance between conductors that determines the associated field levels, but also the phases of conductors affect the final solution. These results were obtained after execution time of only 0.03 s and 12 iterations in the case of considering ice and wind effects, and after 0.02 s and 9 iterations in the case of neglecting ice and wind effects.

5.2. Example 2: Single Circuit 132 kV Horizontal Line

The three conductors are placed on a horizontal line as shown in Fig. 3 for the unoptimized (existing) line and the optimized lines. The currents in the conductors are 485, 472, and 488 A for phases A, B, and C respectively [21]. Magnetic and electric field values are plotted in Fig. 4 where optimized cases show significant decrease compared to the unoptimized case as shown in Table 1. In this example, the optimization process has kept the conductors configuration (horizontal) as well as the phase sequence as shown in Fig. 3. In fact, only the distances between conductors were altered to obtain minimum fields. However, this is not true in all cases as evident from the previous example. The computer program needed execution time of 0.23 s and 1000 iterations to obtain these results in the case of considering ice and wind effects, whereas in the case of neglecting ice and wind effects, 0.24 s and 1000 iterations were needed.

Table 1. Reduction percentages of magnetic and electric fields for optimized lines compared with existing unoptimized line in all examples.

Transmission line description	**Magnetic Field Reduction (with ice & wind)**	**Electric Field Reduction (with ice & wind)**	**Magnetic Field Reduction (without ice & wind)**	**Electric Field Reduction (without ice & wind)**
Example 1: Single Circuit 132 kV Vertical Line	38.71%	27.87%	79.66%	53.57%
Example 2: Single Circuit 132 kV Horizontal Line	42.5%	39.22%	80.31%	74.74%
Example 3: Single Circuit 132 kV Triangular Line	40.32%	45.304%	84.6%	80.56%
Example 4: Double Circuit 132 kV Parentheses Line	59.13%	58.3%	95.7%	96.76%
Example 5: Double Circuit132 kV Horizontal Line	37.74%	27.061%	82.3%	73.35%
Example 6: Double Circuit 380 kV Vertical Line	80.86%	84.1%	96.86%	97.2%
Example 7: Double Circuit 230 kV Delta Line	76.935%	76.58%	92.74%	89.4%

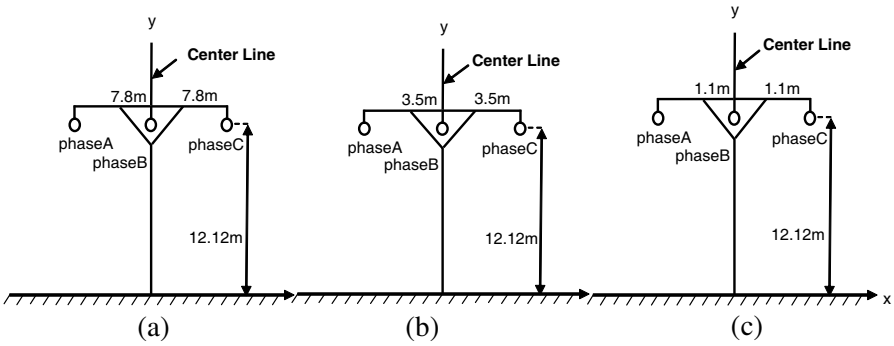

Figure 3. Conductor arrangements for 132 kV overhead horizontal single circuit transmission line with 485, 472, and 488 A in the phases A, B, and C respectively (Example 2). (a) Existing line. (b) Optimized line with considering ice and wind effects. (c) Optimized Line without considering ice and wind effects.

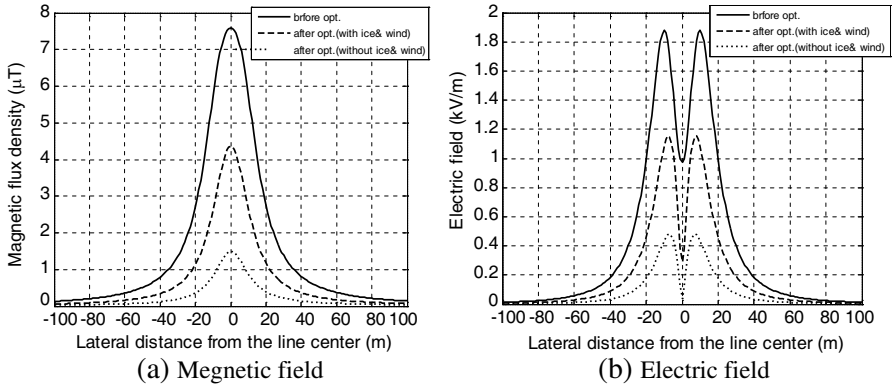

Figure 4. Profile of the magnetic and electric fields under an overhead single circuit horizontal line at 1 m above the ground for the three conductor arrangements in Fig. 3 (Example 2).

5.3. Example 3: Single Circuit 132 kV Triangular Line

The conductors are arranged as shown in Fig. 5 for the line before (existing) and after optimization. The current in each conductor is 35.5 A [21]. Calculated magnetic and electric field values at different lateral locations from the tower were much lower for the optimized lines as compared with the existing unoptimized line as is clear from Fig. 6 and Table 1. The optimized lines have different configurations than

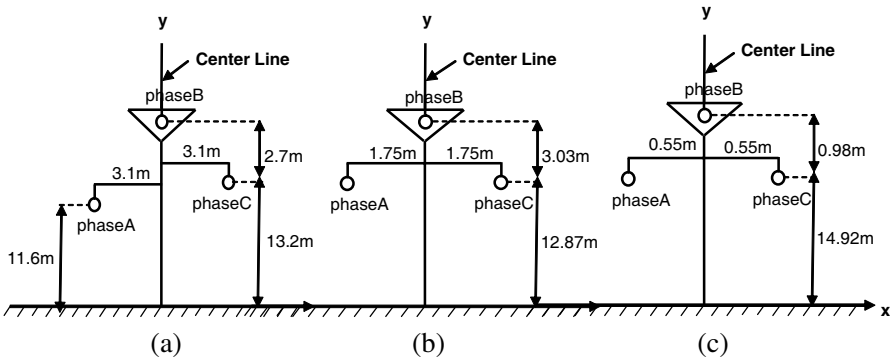

Figure 5. Conductor arrangements for 132 kV overhead triangular single circuit line with 35 A in each phase (Example 3). (a) Existing line. (b) Optimized line with considering ice and wind effects. (c) Optimized line without considering ice and wind effects.

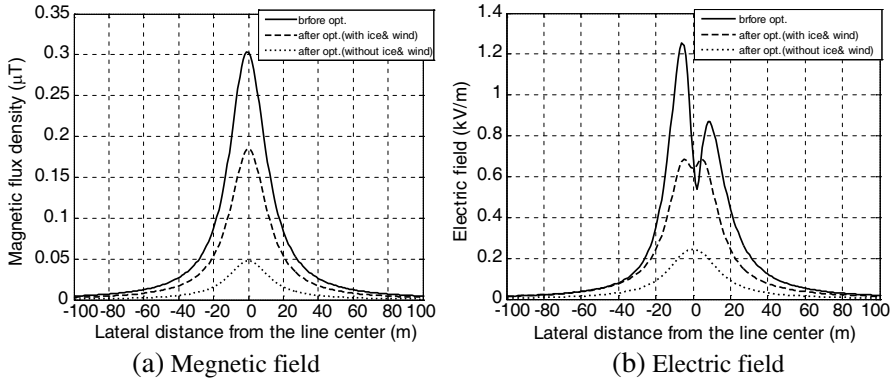

Figure 6. Profile of magnetic and electric fields of 132 kV overhead single circuit triangular line at 1 m above ground for the three conductor arrangments in Fig. 5 (Example 3).

the existing (unoptimized) line, but all lines in Fig. 5 have the same phase sequence. For both cases of considering and neglecting wind and ice effects, the program execution time was 0.01 s and only 1 iteration was needed.

5.4. Example 4: Double Circuit 132 kV Parentheses Line

The current in each phase of the left circuit is 91 A, and the current in each phase of the right circuit is 104 A [21]. For the existing line shown

in Fig. 7(a), the phase is the same in both circuits. The optimized lines have different phase sequences as well as different conductor configurations as shown in Figs. 7(b) and 7(c). The results of running the PSO algorithm are shown in Fig. 8 and in Table 1 for the two cases with considering ice and wind effects and without, where optimized cases show lower magnetic and electric fields than the original line. The program execution time in the case of considering the ice and

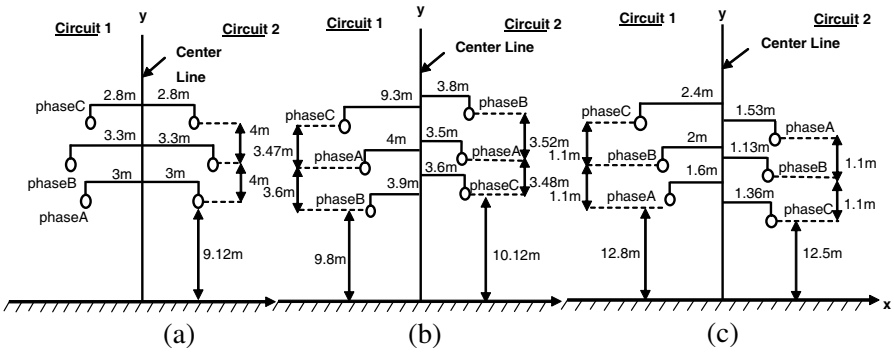

Figure 7. Conductor arrangements for 132 kV overhead double circuit Parentheses transmission line with 91 and 104 A, in each phase of circuit 1 and circuit 2 respectively (Example 4). (a) Existing line. (b) Optimized line with considering ice and wind effects. (c) Optimized line without considering ice and wind effects.

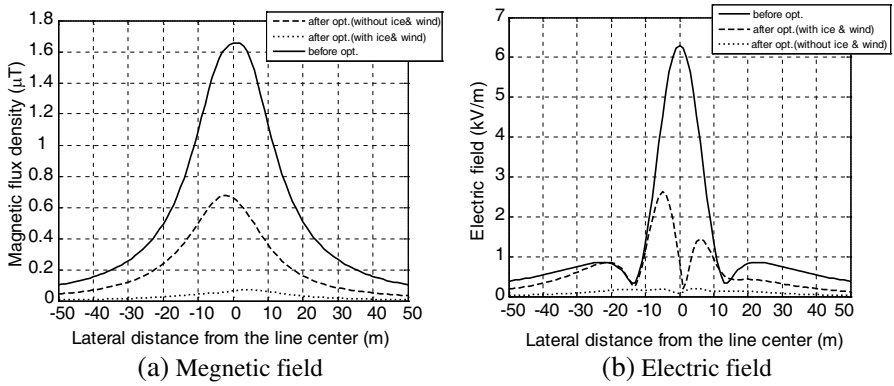

Figure 8. Profile of the magnetic and electric field under 132 kV overhead double circuit parentheses line at 1 m above the ground for the three conductor arrangments in Fig. 7 (Example 4).

wind effects was 0.28 s and the number of iterations was 1000, while in the case of neglecting the effects of ice and wind the time was 0.07 s and iterations were 19.

5.5. Example 5: Double Circuit 132 kV Horizontal Line

Each conductor in this transmission line consists of two bundles separated by 18 inches as shown in Fig. 9. The left circuit in the transmission line has a current of 246 A, whereas a current of 226 A is passing through the right circuit [21]. The phase sequences and conductor configurations of the optimized lines are different from the existing line as evident from Fig. 9. Minimizing both electric and magnetic fields for both cases with and without the effect of ice and

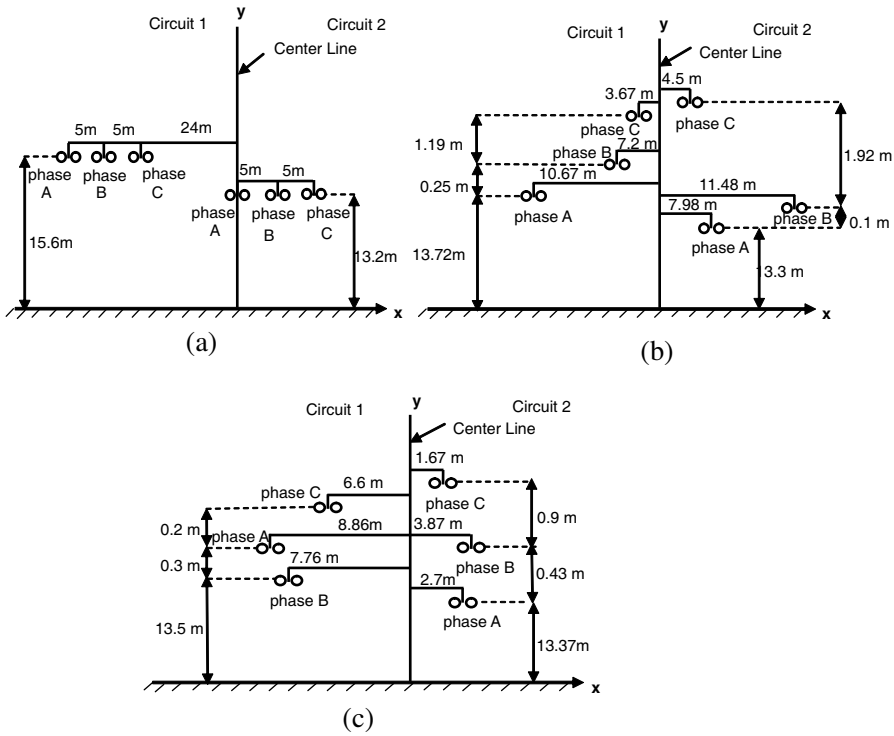

Figure 9. Conductor arrangements for 132 kV overhead double circuit horizontal transmission line with 246 and 226 A, in each phase of circuit 1 and circuit 2 respectively (Example 5). (a) Existing line. (b) Optimized line with considering ice and wind effects. (c) Optimized line without considering ice and wind effects.

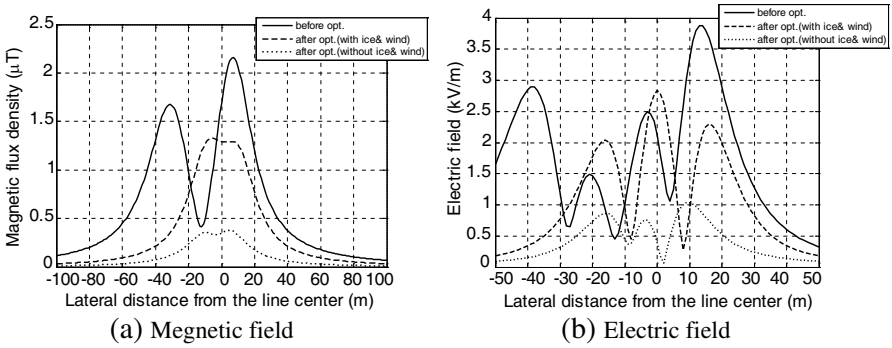

(a) Megnetic field (b) Electric field

Figure 10. Profile of the magnetic and electric fields of 132 kV overhead double circuit horizontal line at 1 m above the ground for the three conductor arrangements in Fig. 9 (Example 5).

wind, we can notify the big decrement in the EMF values as compared with the exiting line, as can be seen from Fig. 10 and Table 1. The execution time for the program to obtain the optimum configurations was 0.25 s and number of iterations was 1000 in the case of considering the ice and wind effects, while in the case of neglecting these effects the time was 0.09 s and iterations were 78.

5.6. Example 6: Double Circuit 380 kV Vertical Line

The current in all phases of the lines shown in Fig. 11 is 855 A [30]. Electric and magnetic fields were simultaneously minimized for both cases of considering ice and wind effects, and neglecting effects of ice and wind. It is clear from Fig. 12 and Table 1 that the fields of the optimized configurations are considerably less than the fields of the existing line. Although the original (existing) line is vertical with the same phase sequence for both circuits, the optimized lines have different configurations and different phase sequences. The optimized results consumed 0.08 s as program execution time, and 44 iterations in the case of considering the effects of ice and wind, whereas in the case of neglecting these effects the time of executing the program was 0.04 s and iterations were 13.

5.7. Example 7: Double Circuit 230 kV Delta Line

Each conductor in this transmission line consists of two bundles spaced by 18 inches, and the current passing through all the phases is 740 A [31]. The existing unoptimized line and the optimized lines

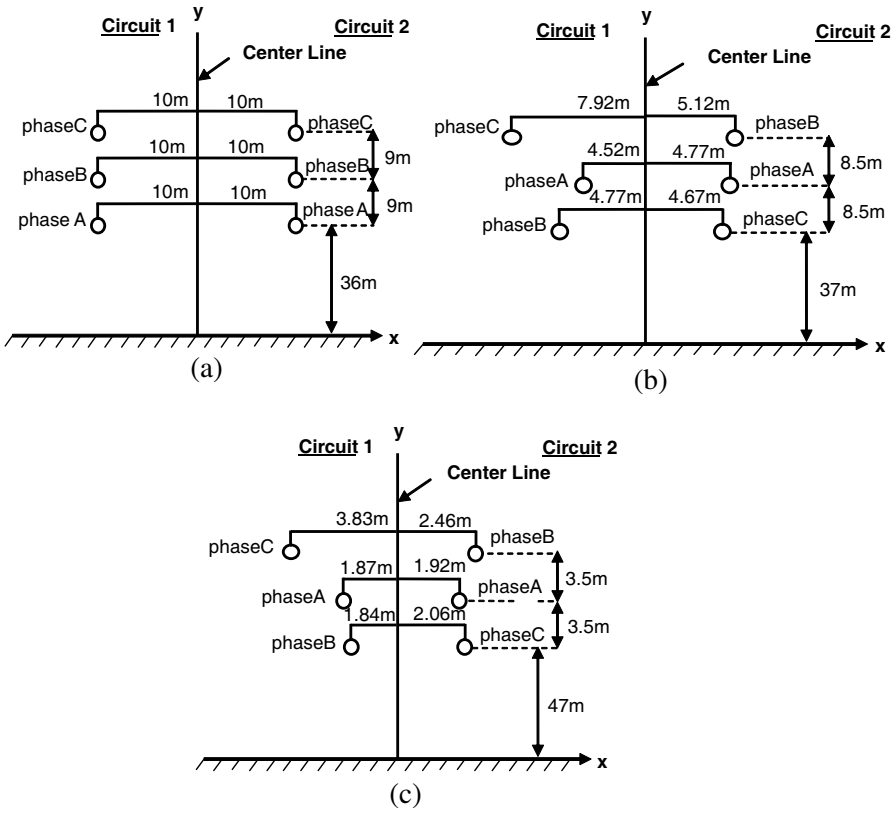

Figure 11. Conductor arrangements for 380 kV overhead double circuit vertical transmission line with 855 A in each phase (Example 6). (a) Existing line. (b) Optimized line with considering ice and wind effects. (c) Optimized line without considering ice and wind effects.

are shown in Fig. 13. While the configurations of the optimized and existing lines are the same, their phase sequences are not the same. Electric and magnetic field values calculated at different lateral locations from the tower for the existing and optimized configurations are plotted in Fig. 14. The optimized lines have lower fields than the existing line as is clear from Fig. 14 and Table 1. The optimized configurations consumed 0.28 s for the program execution and the iterations were 1000 in the case of considering the effects of ice and wind, while in the case of neglecting the effects of ice and wind the execution time was 0.11 s and the iterations were 92.

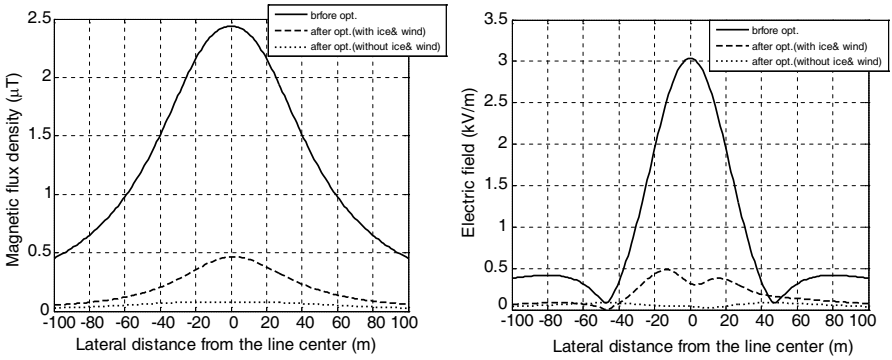

(a) Megnetic field (b) Electric field

Figure 12. Profile of magnetic and electric fields under 380 kV overhead double circuit vertical line at 1 m above ground for the three conductor arrangments in Fig. 11 (Example 6).

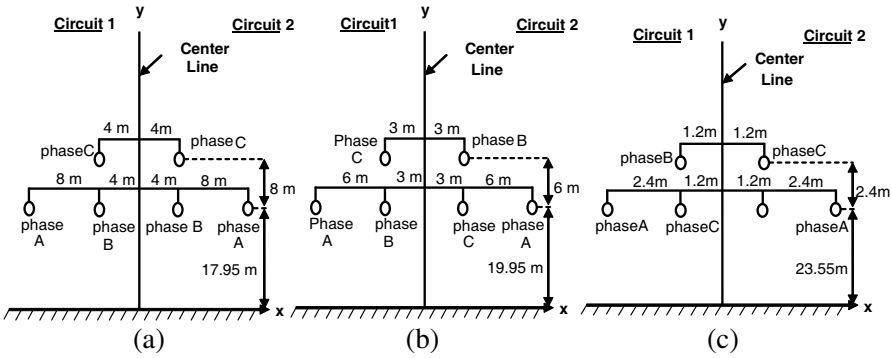

(a) (b) (c)

Figure 13. Conductor arrangements for 230 kV overhead double circuit delta transmission line with 740 A in each phase (Example 7). (a) Existing line. (b) Optimized line with considering ice and wind effects. (c) Optimized line without considering ice and wind effects.

6. COST DISCUSSION

Although the matter of the health effects of electromagnetic fields is controversial, the precautionary principle calls for taking an appropriate action when the scientific information about the risk is not enough. Rearrangement of transmission line conductors was used in this research to reduce EMFs, so we should estimate the cost of using this solution, to know if it's financially acceptable or not. In

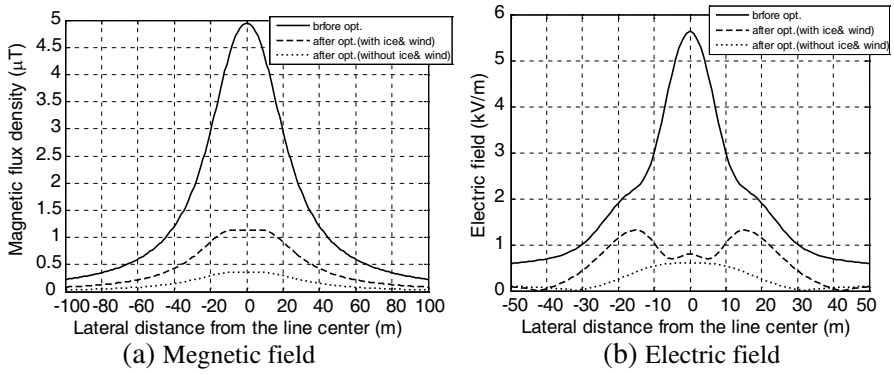

Figure 14. Profile of the magnetic and electric field under 230 kV overhead double circuit delta line at 1 m above the ground for the three conductor arrangments in Fig. 13 (Example 7).

Figure 15. Some views of the study area in Amman, residents are directly under the high voltage line.

this section, we will present some cost estimations made in literature, which we used to compare the cost of transmission line conductors rearrangement with the cost of non-reducing EMFs.

The value of statistical life "VSL" was estimated by California Department of Health Services (CDHS) and the Public Health Institute (PHI) to be $5 million per fatality (measured in 1998 dollars) related to electromagnetic fields exposure, and the value of illness "VOI" was estimated to be $200,000 per illness (measured in 1998 dollars) [23]. Assuming that the annual profit rate is 4%, then VSL equals $8 million per fatality (in 2010 dollars), and VOI equals $320,206/illness (in 2010 dollars).

We made a study to identify the populations living near and also directly under a high voltage 132 kV transmission line passing through a suburban area in the North of Amman in Jordan, as shown in Fig. 15. We took a segment of 3 km of the transmission line, and counted people

and houses within a buffer zone of 100 m on either side from the line center. By direct counting, we found that 1620 housing units are in this buffer zone, and we calculated the number of individuals by multiplying the number of housing units by the average family size given by Department of Statistics (DOS) of Jordan which is equal to 5.3 persons/family, thus there are approximately 8586 individuals within the buffer zone of the transmission line. Based on estimates in [23], we assume that 13 fatalities in addition to 65 illnesses per year are expected to occur among the 8586 individuals living near the transmission line due to EMFs exposure. Using the estimations of VSL and VOI above, the annual cost of fatalities is \$104 million/year (in 2010 dollars), and the annual cost of illnesses is \$20.8 million/year (in 2010 dollars). We can calculate the net present value (NPV) in 2010 dollars for 30 years which is the average lifetime of the overhead transmission line, which amounts to \$1.9024 billion for fatalities in addition to \$380.47 million for illnesses, so the total NPV for non reducing EMFs is \$2.2829 billion in 2010 dollars.

On the other hand, the cost of rearranging a transmission line conductors per mile to reduce EMFs was estimated by the United States Accounting Office (GAO) to be \$90,000/mile (in 1994 dollars), as a result of a study made on replacing conventional transmission line design by a delta design [24]. This cost corresponds to \$168,568/mile in 2010 dollars. Thus the cost of rearranging the 3 km segment of transmission line is estimated to be \$314,229.

It's clear that the cost of transmission line conductors' rearrangement is much less than the cost of non reducing EMFs.

7. CONCLUSION

Rearranging the overhead transmission lines' conductors using PSO can give big reductions in magnetic and electric fields. According to the examples in this paper, magnetic and electric fields reductions can reach up to 81% and 84%, respectively, in the case of considering the effects of ice and wind, and the reduction percentage can reach up to 97% for both magnetic and electric fields in the case of neglecting the effects of ice and wind. Cost estimates for a study area in Amman, where a high voltage line passes over and near residents, favor the electromagnetic fields reduction through rearranging the line conductors.

REFERENCES

1. Van Loock, W., "Elementary effects in humans exposed to electromagnetic fields and radiation," *5th Asia-Pacific Conf. on Environmental Electromagnetics (CEEM)*, 221–224, Belgium, 2009.
2. Neutra, R. R., V. DelPizzo, and G. M. Lee, "An evaluation of the possible risks from electric and magnetic fields (EMFs) from power lines, internal wiring, electrical occupations and appliances," *California EMF Program*, Oakland, California, USA, Jun. 2002.
3. Florea, G. A., A. Dinca, and A. Gal, "An original approach to the biological impact of the low frequency electromagnetic fields and proofed means of mitigation," *IEEE Bucharest Power Tech. Conf.*, 1–8, Romania, 2009.
4. IARC, "Static and extremely low-frequency (ELF) electric and magnetic fields: IARC monographs on the evaluation of carcinographic risks to humans," Vol. 80, International Agency for Research on Cancer, Lyon, France, 2002.
5. Rao, S., A. Sathyanarayanan, and U. K. Nandwani, "EMI problems for medical devices," *IEEE Proceedings of the International Conference on Electromagnetic Interference and Compatibility*, 21–24, India, Dec. 1999.
6. Shwehdi, M. H., "A practical study of an electromagnetic interference (EMI) problem from saudi arabia," *2004 Large Engineering Systems Conference on Power Engineering*, 162–169, Canada, Jul. 2004.
7. ICNIRP (The international commission on non-ionizing radiation protection), "Guidelines for limiting exposure to time-varying electric, magnetic and electromagnetic fields (up to 300 GHz)," *Health Physics*, Vol. 74, No. 4, 494–522, Apr. 1998.
8. Hossam-Eldin, A., K. Youssef, and H. Karawia, "Measurements and evaluation of adverse health effects of electromagnetic fields from low voltage equipments," *12th International Middle-east Power System Conf. (MEPCON)*, 436–440, Egypt, 2008.
9. Swanson, J., "EMF exposure standards applicable in Europe and elsewhere," Environment & Society Working Group, Union of the Electricity Industry — EURELECTRIC, Belgium, May 2003.
10. Wassef, K., V. V. Varadan, and V. K. Varadan, "Magnetic field shielding concepts for power transmission lines," *IEEE Transactions on Magnetics*, Vol. 34, No. 3, 649–654, May 1998.
11. Celozzi, S. and F. Garzia, "Active shielding for power-frequency magnetic field reduction using genetic algorithms optimization,"

IEE Proceedings — Science, Measurement and Technology, Vol. 151, No. 1, 2–7, Jan. 2004.

12. Canova, A. and L. Giaccone, "Magnetic field mitigation of power cable by high magnetic coupling passive loop," *20th International Conference and Exhibition on Electricity Distribution*, 1–4, Prague, Czech Republic, Jun. 2009.
13. Nourai, A., A. Keri, and C. Shih, "Shield wire loss reduction for double circuit transmission lines," *IEEE Trans. on Power Delivery*, Vol. 3, No. 4, 1854–1864, 1988.
14. Kalyuzhny, A. and G. Kushnir, "Analysis of current unbalance in transmission systems with short lines," *IEEE Transactions on Power Delivery*, Vol. 22, No. 2, 1040–1048, 2007.
15. Electric Power Research Institute, *EPRI Transmission Line Reference Book: 115–345-kV Compact Line Design*, Electric Power Research Institute, USA, 2008.
16. Al Salameh, M. S. H., I. M. Nejdawi, and O. A. Alani, "Using the nonlinear particle swarm optimization (PSO) algorithm to reduce the magnetic fields from overhead high voltage transmission lines," *IJRRAS: International Journal of Research and Reviews in Applied Sciences*, Vol. 4, No. 1, Jul. 2010.
17. Kennedy, J. and R. C. Eberhart, "Particle swarm optimization," *Proceedings of IEEE International Conference on Neural Networks*, 1942–1948, Piscataway, NJ, 1995.
18. Pedersen, M. E. H. and A. J. Chipperfield, "Simplifying particle swarm optimization," *Applied Soft Computing*, Vol. 10, No. 2, 618–628, 2010.
19. Premalatha, K. and A. Natarajan, "Hybrid PSO and GA for Global Maximization," *Int. J. Open Problems Compt. Math. International Center for Scientific Research and Studies*, Vol. 2, No. 4, Dec. 2009.
20. Moradi, A. M. and A. B. Dariane, "Particle swarm optimization: Application to reservoir operation problems," *IEEE Int. Advance Computing Conf. (IACC 2009)*, 1048–1051, Patiala, 2009.
21. Garrido, C. and A. Otero, "Low frequency magnetic fields from electrical appliances and power lines," *IEEE Transactions on Power Delivery*, Vol. 18, No. 4, 1310–1319, Oct. 2003.
22. Olsen, R., "Field computation models: A: Calculation of ELF electric and magnetic fields air," *Field Computation Models*, Available from URL ftp://ftp.emf-data.org/pub/emf-data/symposium98/topic-06a-synopsis.pdf.
23. Winterfeldt, D., "California department of health services

and the public health institute, power grid and land use policy analysis 2001, final report," Dec. 2009, Available from URL http://www.ehib.org/emf/pdf/Chapter09-ValueofInformation.pdf.

24. United States General Accounting Office, "Electromagnetic fields: Federal efforts to determine health effects are behind," GAO Resources, Community, and Economic Development Division, Washington, 1994.
25. Luwen, X., H. Xingzhe, L. Yongming, and L. Changsheng, "Study on shielding optimization for power-frequency electric field under over head transmission line," *Symposium on Radio Interference and Electromagnetic Compatibility of Substation ('08 EMI)*, Zhuhai, China, Nov. 2008.
26. Robinson, J. and Y. Rahmat-Samii, "Particle swarm optimization in electromagnetics," *IEEE Transactions on Antennas and Propagation*, Vol. 52, No. 2, 397–407, 2004.
27. Luo, J. X., D. Wu, Z. Ma, T. Chen, and A. Li, "Using PSO and GA to optimize schedule reliability in container terminal," *International Conference on Information Engineering and Computer Science (ICIECS)*, 1–4, Wuhan, China, Dec. 19–20, 2009.
28. Tian, D. P. and N. Q. Li, "Fuzzy particle swarm optimization algorithm," *International Joint Conference on Artificial Intelligence (JCAI '09)*, 263–267, Hainan Island, China, Apr. 25–26, 2009.
29. Saadat, H., *Power System Analysis*, 2nd edition, McGraw Hill, USA, 2002.
30. Mazzanti, G., "Current phase-shift effects in the calculation of magnetic fields generated by double-circuit overhead transmission lines," *IEEE Power Engineering Society General Meeting*, Vol. 1, 413–418, New York, USA, Jun. 2004.
31. Bakhashwain, J. M., M. H. Shwehdi, U. M. Johar, and A. A. AL-Naim, "Magnetic fields measurement and evaluation of EHV transmission lines in Saudi Arabia," *Proceedings of the International Conference on Non-ionizing Radiation at UNITEN (ICNIR 2003), Electromagnetic Fields and Our Health*, Malaysia, Oct. 20–22, 2003.